

**Starvation response in mouse liver shows strong correlation
with lifespan prolonging processes**

**Matthias Bauer(1,2), Anne C. Hamm(1,2), Melanie Bonaus(2), Andrea Jacob(3),
Jens Jaekel(4), Hubert Schorle(3), Michael J. Pankratz(2,5), and Joerg D.
Katzenberger(2)**

(1) The two authors contributed equally

(2) Institut fuer Genetik, Forschungszentrum Karlsruhe, Postfach 3640, 76021 Karlsruhe,
Germany

(3) Institut fuer Pathologie, Universitaet Bonn, Sigmund Freud Str. 25, 53127 Bonn,
Germany

(4) Institut fuer Angewandte Informatik, Forschungszentrum Karlsruhe, Postfach 3640,
76021 Karlsruhe, Germany

(5) Corresponding author

E-mail: michael.pankratz@itg.fzk.de

Abbreviated title: Mouse liver starvation response

ABSTRACT

We have monitored global changes in gene expression in mouse liver in response to fasting and sugar fed conditions using high density microarrays. From approximately 20,000 different genes, the significantly regulated ones were grouped into specific signaling and metabolic pathways. Striking changes in lipid signaling cascade, insulin and DHEA hormonal pathways, urea cycle and S-adenosylmethionine based methyl transfer systems, and cell apoptosis regulators were observed. Since these pathways have been implicated to play a role in the aging process, and since we observe significant overlap of genes regulated upon starvation with those regulated upon caloric restriction, our analysis suggests that starvation may elicit a stress response which is also elicited during caloric restriction. Therefore, many of the signaling and metabolic components regulated during fasting may be the same as those which mediate caloric restriction dependent lifespan extension.

Key words: microarray analysis, nutrient response, caloric restriction, metabolic signaling, aging/longevity

INTRODUCTION

The health consequences of abnormal metabolic regulation are enormous. These include in born errors of metabolism that affect specific enzymes of a biochemical reaction and defects in hormone systems, such as diabetes, that coordinate nutrient utilization (59). In addition, changes in modern diet and lifestyle have drastically increased unwanted consequences in body metabolism even in non-diseased condition, as seen in the dramatic increase in obesity and cardiovascular disorders (25, 84). While some of the metabolic defects can be controlled by appropriate dietary modification, e.g., avoiding food containing high levels of phenylalanine can prevent fatal consequence of phenylketonurea, molecular mechanisms underlying the physiologic response to different nutrient conditions are largely unknown. The controversies surrounding the relative efficacy of different diets and diet supplements to battle a wide spectrum of health conditions attest to this lack of knowledge (69). On the other end of the health spectrum, evidence is accumulating that restricting caloric intake can slow down the effects of aging and increase lifespan in all model organisms tested to date (41, 63). This has been attributed to several factors, including oxidative stress, genome integrity and endocrine signaling. To understand how diet affects progression of diseases and aging, one of the goals would be to identify the metabolic pathways affected by altered nutrient conditions and the underlying genetic and signaling control mechanisms that regulate them.

The major reactions of the biochemical pathways leading to the metabolism of essential nutrients have been worked out (46). These have come mostly through studying the

substrates and products of the reactions and the enzymes catalyzing them. Regulations of the reactions have furthermore focused on the activity and specificity of the enzymes in terms of allosteric control and post-translational modifications. Thus, one way to study changes in flux through a particular metabolic pathway in response to altered diet would be to measure substrate and product concentrations of a particular reaction. This however is not yet feasible for multicellular organisms on a large scale. A complementary approach is through analysis of genes that encode these enzymes using recently developed genomic technologies. Although altering enzyme levels may not necessarily result in altering flux through that pathway, significant alterations in the expression of the enzyme encoding genes may reflect responsive flux changes. In addition, this approach may identify molecules that regulate specific metabolic pathways, such as transcription factors or components of signal transduction cascades. We have already utilized such a strategy to study nutrient regulated gene regulation in *Drosophila* (85). Based on these considerations, we have analyzed nutrient dependent gene expression changes using microarrays in mouse liver.

In mammals the liver plays a key role in coordinating body metabolism in response to dietary conditions. Much of the regulatory effects occur initially in the liver, which then modulates the activities of other organs regarding nutrient utilization and metabolism. We have carried out a comprehensive microarray gene profiling analysis in mouse liver under fasting and under sugar conditions. Numerous studies have utilized microarrays to study nutrient regulation of gene expression, but these differ with respect to the number of genes, type of microarrays, organs tested and the specific nutrient conditions. Our study

provides the most comprehensive gene profiling to date on the patterns of gene expression under fasting and sugar conditions in the same experimental setup, representing some 20,000 different mouse genes. Our results pinpoint several metabolic and signaling pathways that may be part of a global regulatory response to food restriction. These pathways may be important for providing insights into understanding nutrient dependent disorders. Furthermore, our analysis reveals a connection between starvation response and those which may slow aging. Our results suggest that many of the physiological pathways operating upon starvation underlie those operating during lifespan extension brought on by caloric restriction.

MATERIALS AND METHODS

Microarray Production

20,160 PCR products were amplified from a collection of cDNAs (Array Tag, set A and B) that was made by LION bioscience AG, Heidelberg, Germany. These cDNAs (150 to 700 bp) were derived from 3' end of ESTs, cloned and sequenced by the company. We amplified the inserts using primers designed from the vector sequence flanking the insert (primer sequence provided by LION bioscience). The PCR products were cleaned using Millipore 96-well filtration plates (HPPV, 0.45 μ m, clear) and transferred into 384-well plates, dried and resuspended in 1.5M betaine/1x phosphate printing buffer (150mM sodium phosphate, pH 8.5). The amplified cDNA products (200 - 500 ng/ μ l) were spotted in duplicates in two separate subarrays using a Genemachines (San Carlos, CA, USA)

Omnigrid 100 and Telechem (Sunnyvale, CA, USA) SMP3 pins on Corning (Corning, NY; USA) CMT-GAPS II slides.

Nutrient Conditions

Mice used in this study were 129/sv males, 8-15 weeks of age, which were housed individually and received water ad libitum. 12 animals were taken for the 24 hour experiment, in two batches of six animals each (three fasted, 3 normal fed controls). Total RNA and polyA RNA were prepared for each sample probe separately, and equal amounts of polyA RNA from each batch and each condition were pooled, i.e., three animals per pool. A fifth pool was made in which all starved animals were included, as well as a sixth pool that contained all normal controls. Pool 1/2 (normal fed) was hybridized the same manner against pool 3/4 (24 hour starved), and pool 5 (starved) was hybridized against pool 6 (normal fed). For experiments on 48 hour nutrient condition, 10 normal fed and 10 starved animals were used (distributed in groups of three, three and four per condition). Pooling was done as described above for each group and 8 arrays were hybridized per group (with dye swap). In the third set up, 10 animals received a sugar solution (40% sucrose and 10% glucose) and water ad libitum, and these were compared to 10 normal fed animals. Pooling and hybridizations were done as described for 48 hour starved experiment.

RNA preparation, Labeling and Hybridization

Mice were killed by CO₂ asphyxiation. The livers were snap-frozen in liquid nitrogen and stored at -80 degrees C. Total RNA was prepared using the Nucleospin RNA L kit

(Macherey-Nagel, Dueren, Germany), with an additional step in which the final eluate was used for a subsequent elution step. PolyA RNA was extracted with the Ambion (Ambion Inc, Austin, USA) Purist kit according to the manufacturer's protocols. Equal amounts of polyA RNA were pooled to generate normal or starved or sugar pools of all animals. These were hybridized against each other on 24 arrays for the 24 h and 48 starvation experiments each and on 12 chips for the 48 h sugar experiment. Half of the arrays were hybridized as dye-swaps. Labeled cDNA was synthesized from 1.5 μ g polyA RNA using the Amersham (Amersham Europe, Freiburg, Germany) direct cDNA labeling kit. Removal of the unincorporated dyes and concentration of the target were done with Microcon 30 (Millipore, Bedford, MA) spin columns according to the manufacturer's instructions. The concentrated probes were hybridized to the microarray in 1x dig easy hyb buffer (Hoffman-la Roche, Basel, CH) overnight at 42 degrees C.

Microarray scanning

Arrays were scanned using the dual laser scanner Axon 4000B and the corresponding software Genepix 4 (Axon Inc., Union City, CA, USA). Both channels (532 nm for Cy3 and 635 nm Cy5) were scanned in parallel and stored as 16 bit tiff files. The absolute intensity values span the range from 0 to 65,535. The scans were performed with a resolution of 10 μ m. From each spot with a mean diameter of 100 μ m, 100 data pixels were recorded. Individual local background area around the spots were defined, which included approximately 400 pixels and excludes neighboring spots. For each channel, the raw data was calculated as the median intensity of all foreground pixels with respect to all background pixels.

Each array was scanned three times (low, medium and high scan) with different signal amplification factors (voltage settings of the photo multiplier tubes), but with the same laser power. The channels for Cy3 and Cy5 were balanced in each scan for approximately the same intensity profile. In the low scan no spot was saturated, in the high scan the signal amplification for Cy5 was set to approximately 80% of maximum and the Cy3 amplification was adjusted to this. The settings used in the medium scan lie between the low and the high scan. This method for scanning has several advantages. In the low scan where no spot is in saturation, it is possible to calculate the real ratio for genes with high expression levels; however, those with a low expression level are most likely not recognized. In order not to lose these, a high scan is made; in this case, the information on the saturated spots is lost, so the two scans complement each other. The medium scan produces additional values for subsequent calculations. By scanning the arrays three times, errors which occur while recording and which might increase the error factor in the normalization are averaged.

Data Processing and Normalization

The data processing was automated in a Visual Basic/Excel (Microsoft) program, which integrates the following steps. Raw data are derived from the result files generated by scanning and picture analysis software Genepix. The spot diameter is to lie in the range from 80 to 120 μm otherwise these spots are not included in analysis. From the pixel to pixel ratios between the foreground values of both colors, the standard deviation (SD) is calculated. Those spots which show a ratio SD of higher than 3 are excluded from analysis due to inconsistency. The foreground signal of each spot is corrected by

subtracting the corresponding local background. Resulting values which are lower than the background are replaced by the background value. This defines the minimum measurement threshold as the background and avoids calculations of completely wrong ratios, e.g., if the background corrected value for one channel is close to zero. Spots are marked as saturated in one channel if more than 10% of the foreground pixels are at the highest absolute value. From the unsaturated data points of all three scans, linear regression between the low and medium, and between low and high scans, are calculated for both colors. Taking these regressions, the values of saturated spots are replaced by estimated ones which reflect the real intensity.

The generated data set of each scan is normalized afterwards based on the intensity-dependent methods as described by Yang et al. (80). The ratios are calculated as log₂ transformed values: $M = \log_2(Cy5/Cy3)$. Number describing the spot intensity $A = \log_2 \sqrt{Cy5 * Cy3}$ is calculated according to Yang et al (80). A within pin-tip group loess fit to the MA-plot was made. The loess scatter plot smoother performs robust locally fits using a tricube function to weight the values relative to the median point in the intensity interval. An interval size of 20% was chosen, which corresponds to 180 data points in a pin-tip group containing 30 by 30 spots. After combining the normalized data from all blocks the data sets of all scans are additionally normalized using a global approach. The normalization was performed so that the sum of all log transformed ratios (M) is 0.

All statistical normalizations are based on the assumption that (1) the majority of genes are not changed in their expression and (2) that the overall up and down regulations statistically compensate each other in sum. Taking this into account, the standard deviation in the ratios of the stable genes (80% of the most unchanged genes) could be

seen as the measurement noise of the array experiments. To be able to compare the different scans and different normalized microarrays, the SD of the stable genes ratios was adjusted to a medium estimated value of 0.2, which is dependent on the used array system. This value does not influence the subsequent statistical analysis because the normal distribution of the data is not changed. For each microarray the normalized and adjusted log ratios of the three scans are averaged. On the used arrays, two identical subarrays are present; thus the data were divided block wise into two sets. Each set is taken afterwards as a distinct element in the statistical test. The data are stored in a relational database using the Filemaker pro software (Filemaker Inc, Santa Clara, CA USA).

Statistical Analysis

RNA was hybridized to minimum 12 (for 48 h sugar) replicate microarrays, giving rise to 24 data points for each gene. The criteria for a gene to be considered for statistical analysis in a t-test was that at least 16 of 24 are present (i.e., the data was derived from at least 8 different arrays). In subsequent examinations, only those genes whose ratios placed it in the 99.5% confidence interval were included. RT-PCR analysis was performed for nine genes and all were consistent with the microarray data. The primer sequences used are listed below; beta actin was used as control. Cog2 was used as additional control as this showed no regulation from the microarray analysis. These represented both up regulated (Cyp4a14, Ela2, Fkbp5, Gadd45b, Got1, Igfbp1 and Lepr) and down regulated (Car3 and Temt) genes upon starvation and all but one of the signaling or metabolic pathways are represented by at least one gene.

(gene symbol: sequence forward primer / sequence reverse primer)

beta actin: AAGGCCAACCGTGAAAAGATGA / TGTCAGCAATGCCTGGGTACAT

Car3: TCTGGCCAGTTAGAAAGCCTGTG / GTCCGCATACTCCTCCATACCC

Cog2: TTCAGAGTGGACATGGGGACAA / CACCAGCCACACTTGTCGATTT

Cyp4a3: GCCTGTTACCCCTCATAACCA / CGCCAACCTGCATTTCTACACA

Ela2: GTCTCCCTGCAGGTCCTTTTCT / GTTGGAGACCCTGGTGAAGACG

Fkbp5: GTGTCCATGCATCAAGCCAAAG / ATACCAGTCTCCTTGGCCCACA

Gadd45b: GAAGGCCTCCGACACTTCTGGT / GAGTGGGTCTCAGCGTTCCTCT

Got1: CTGACCGTGGTTCGGAAAAGAGT / TCCAACAGGCTCTAACCCAGAA

Igfbp1: ACATCCCTGGATGGAGAAGCTG / AGCTTTCCACGTTTCAGCTTTGG

Lepr: GCCAGTCTTTCCGGAGAATAACC / CTGCTGCTCAGGGGATAAGCAC

Temt: CTGACTACACCCCGCAGAACCT / GCTGTGGAGCAAGGCTTTACAA

RESULTS

Experimental and Microarray Setup

We performed experiments to identify genes regulated under 24 and 48 hours fasting, as well as 48 hours only on sugar (Table 1). The sugar treatment was used as a first step to see if the starvation effect was due to a simple lack of energy source or whether some other nutrient signals, for example amino acids, could be responsible. For 24 hours fast, a total of 12 mice were used (6 normal, 6 starved) and hybridized to 24 arrays. For 48 hours

fast, a total of 20 mice were used (10 for normal and 10 for starved) and hybridized to 24 arrays. For 48 hour sugar fed, a total of 20 animals were used (10 normal and 10 sugar) and hybridized to 12 arrays. Each microarray contains approximately 20,000 PCR products representing different genes printed in duplicates (see Material and Methods). For each experimental condition, dye swaps were performed (Table 1). Scanning of each array was done three times at three different intensities. Normalization was carried out using loess (80). For every experiment, each sample class was hybridized to a minimum of 12 replicate microarrays; since there are two subarrays, there are minimum 24 data points for each experimental setup. Only those genes with 99.5% confidence level by t-test were used (see Material and Methods for details). These data provide a large scale, statistically reliable view of the changes in gene expression in the mouse liver during fasting and sugar fed conditions.

The data on which this paper is based have also been deposited with the NCBI Gene Expression Omnibus (www.ncbi.nih.gov/geo). The sample series GSE853 contains data of the 24h starvation, GSE852 of the 48h starvation and GSE851 of the 48h sugar experiment.

Overview

As a first step, we compared the number of genes regulated in the three conditions (24 hour starvation, 48 hour starvation and 48 hour sugar). As expected, the number of genes increased in going from 24 to 48 hours of starvation. Furthermore, the number of genes regulated under sugar at 48 hours is much lower than starved (Fig 1). This is not

surprising since sugar feeding is a much less radical alteration in diet than total fasting. Furthermore, most of the regulated genes in starvation no longer become regulated to as high a degree when sugar is present. In order to discern which of the gene expression changes might have biologically meaningful consequences, we reasoned that significant alterations in flux through a given metabolic pathway may come about through large changes in single key components and/or a series of smaller changes in different components comprising the pathway. To structure the data, we did not use the common approach of clustering based on expression changes. Instead we grouped the genes in specific metabolic or signaling pathways to obtain a more functional sense of the data.

Fat Metabolism

During fasting, the body breaks down fats to generate energy. As expected, many genes encoding enzymes used in β -oxidation of fatty acids are highly up regulated upon starvation (Table 2). One of the highest up regulated gene in our list encodes a peroxisomal acyl-coenzyme A thioester hydrolase (Pte-2a). This result is consistent with previous results from Northern analysis showing increased expression of Pte-2a upon fasting (28). The gene encoding carnitine acetyltransferase (crat), which is required for transport of fatty acids into the mitochondria for β -oxidation (30, 34), is also up regulated. There is also up regulation of long chain acyl-CoA dehydrogenase gene (Acadl) and peroxisomal enoyl-CoA hydratase gene (Ech1) (18, 38), which are involved in β -oxidation.

Concomitant with up regulation of genes involved in fat breakdown, genes encoding enzymes involved in fat synthesis are down regulated. These include stearoyl-CoA desaturase (Scd1), a key lipogenic enzyme for synthesis of monosaturated oleic acid (52). Knockout of Scd1 gene protected mice against adiposity, demonstrating its importance in fat synthesis (51). A special regulatory effect is observed for the Scd1 gene, namely that it is decreased upon starvation and increased in sugar. There are very few genes which show opposite regulation to this extent in the two nutrient conditions, strengthening the view that Scd1 expression is especially sensitive to sugar and fat metabolism. Other down regulated genes include fatty synthase (Fasn), peroxisomal nudix hydrolase (Nudt7) and butyryl coenzyme A synthetase 1 (Bucs1) (16, 22).

Recently, the gene for Hyplip1 locus, which causes familial combined hyperlipidemia, was identified as thioredoxin interacting protein (Txnip) (4, 76), and this gene is up regulated upon starvation. Interestingly, the Txnip gene is also dramatically up regulated in glucose treated pancreas (60). We also see up regulation of leptin receptor and Fsp27, suggesting their function in fat breakdown in the liver (12, 48). Genes involved in lipid transport are also affected (57). Apolipoprotein A-IV (Apoa4) is up regulated, whereas apolipoprotein 2 gene is down regulated, suggesting that the former has a role in fat breakdown, while the latter has a role in fat synthesis. There is also down regulation of the different serum amyloid A genes (Saa), whose products bind and transport HDLs, as well as numerous esterases (Es).

PXR and CAR nuclear receptors

The breakdown products of dietary lipids, as well as drugs and other xenobiotics, must be detoxified and eliminated. One signaling cascade that performs these functions comprises nuclear receptors which are activated by lipid ligands and regulate target genes that function in lipid metabolism (9). By similar token, catabolism of endogenous fats upon starvation appears to operate through the same signaling cascade. For example, the high up regulation of Pte-2a mentioned above is dependent on PPARalpha, a major fatty acid sensor (28). While the PPARs are not transcriptionally regulated themselves, the PXR and CAR genes, which act as xenobiotic sensors, show increased expression upon starvation (Table 3). These are among the highest regulated transcription factors. Targets of lipid activated nuclear receptor include Cyp enzymes, cytosolic binding proteins and ABC transporters (9), and we also observe strong regulation of these genes (Tables 3 and 4).

Cytochrome P450s, cytosolic binding proteins and ABC transporters

A critical family of proteins that regulate lipid metabolism and detoxification is cytochrome P450s. The expression profiles of the different members of this family represent one of the most striking in our analysis (Table 4). The highest up regulated gene among the 20,000 genes represented, in both 24 and 48 hour starvation, is cytochrome P450 4A14 (Cyp4a14). Disruption of this gene in mice has been shown to cause hypertension (26). Another highly up regulated gene is Cyp17a1, which is involved in

DHEA synthesis from cholesterol (see also Table 7). Among the down regulated genes, cytochrome P450 2C70 (Cyp2c70) is the second most down-regulated gene in our microarray; little is known about the function of this gene, but its strong down regulation upon starvation suggests a role in lipid synthesis. There are two other cytochrome P450s that are highly down regulated. Cyp4f14 may play a role in the inactivation of eicosanoids (37), whereas Cyp7b1 is involved in bile acid synthesis (54).

We have also noted a potentially interesting regulation of cytochrome P450s by aminolevulinic acid. Aminolevulinic acid synthetase (Alas) is the first enzyme in the synthesis of heme, a component of cytochrome P450 (33). Of the aminolevulinic acid produced in the rat liver, as much as 65 % is used for formation of cytochrome P450s. Thus, an increase in ALAS would result in increased heme levels required for increased antioxidant and detoxification function of cytochromes P450s. It is interesting that while the liver expressed Alas1 is up regulated, Alas2, which in literature is known to be red blood cell specific, is down regulated (Table 4). This could mean that as red blood cells become degraded upon nutrient shortage, the freed amino acids and heme become refunneled for cytochrome P450 production.

Among the genes encoding the family of 14-15kb intracellular fatty acid binding proteins, the epidermal specific lipid binding protein (E-FABP/Fabp5) (24, 77) is the most strongly down regulated (Table 3). It is expressed in adipocytes and skin, but its role in the liver has not been characterized. There is also small but significant regulation of other fatty acid binding proteins and ABC transporters, including the down regulation of Abcb11, a

target of farnesoid receptor FXR (15). Some of the others may be targets of lipid activated nuclear receptors PXR and CAR.

Urea cycle and amino acid metabolism

In addition to fat breakdown, prolonged fasting results in the breakdown of endogenous proteins and amino acids in order to generate energy and to reallocate available metabolic resources. In keeping with this, we observe gene expression changes that may reflect an increase in flux through amino acid metabolism and urea cycle (Table 5). For example, the lysosomal cysteine protease cathepsin L (*ctsl*) gene expression is unchanged at 24 hour starvation but becomes up regulated after 48 hours starvation. It has already been reported that the activity and protein level of *ctsl* is increased in starved rats (29), and that a knockout of this gene results in heart defects (66). This up regulation of *ctsl* is completely suppressed by sugar, suggesting that with sufficient energy source, *ctsl* targeted proteins need not to be catabolized. We also observe an up regulation of saccharosine dehydrogenase (*Aass*), which is involved in lysine catabolism: this up regulation is also suppressed in sugar condition. Consistent with this finding, treatment with glucagon has demonstrated increased flux through lysine catabolism pathway (58). There is also down regulation of the gene encoding glutamine synthetase (*Glu1*), a key enzyme in amino acid metabolism. In *E. coli* the enzyme glutamine synthetase is rapidly degraded upon nitrogen starvation (64).

More specifically, we observe a high up regulation of aspartate aminotransferase encoding gene *Got1* (also known as glutamic-oxalacetate deaminase), together with three other genes of the urea cycle, namely arginase (*Arg1*), argininosuccinate lyase (*Asl*) and carbamoyl phosphate synthetase (Fig 2; Table 5). This most likely reflects the need to utilize amino acids as energy source. Remarkably, the four genes up regulated in starvation are all down regulated in sugar condition. This suggests that in the presence of sugar, the body tries to spare protein degradation, resulting in decreased flux through the urea cycle. This pattern is reminiscent of *Scd1* regulation during fat metabolism (see above) and further strengthens the view that flux through the urea cycle is particularly sensitive to nutrient conditions.

We also observe a large down regulation of carbonic anhydrase III gene (*Car3*). It is in fact the highest down regulated gene in our microarray. The carbonic anhydrases are involved in bicarbonate buffering function. This is necessary to maintain acid-base homeostasis since increased amino acid catabolism would create a pH imbalance. On the other hand, it has been reported that *Car3* is found at a much higher level in male than in female mice, in which case the down regulation may reflect a need to suppress synthesis of certain sex hormones.

S-adenosyl methionine cycle and methyl transferases

Several key enzymes of the S-adenosyl methionine (SAM) cycle are up regulated upon starvation (Figure 3, Table 6). SAM plays a critical role in methyl transfer reactions,

including one carbon metabolism. The gene for methionine-adenosyl transferase (Mat1) is the highest up regulated; this enzyme catalyzes the only known biosynthetic pathway for SAM from methionine and is required for proper liver function (42, 43). The regulation of gene encoding betaine-homocysteine methyltransferase (Bhmt) seems to be especially sensitive to different nutrient conditions, since there is a large opposite regulation between starvation (up regulated) and sugar condition (down regulated). This is very similar to of the behavior of Scd1 during fat metabolism. This regulatory pattern of Bhmt may be important for setting homocysteine levels under various nutrient and health conditions (20). For example high homocysteine levels have been associated with heart defects (19, 57). In this context, decreased Bhmt (as observed in sugar condition) would lead to higher homocysteine levels, whereas increased Bhmt (as observed during fasting) would lower homocysteine levels.

Several methyltransferases that utilize SAM are also regulated upon starvation (Table 6). Especially interesting is the gene encoding catechol-O-methyltransferase (COMT), which catabolizes several catecholamines in the liver, including epinephrine and norepinephrin. COMT has been implicated in Alzheimer's disease and aging, as well as in responding to a pain stressor (86). In addition, COMT inhibitors have been used as treatment for Parkinson's and other age related diseases (78, 83) There is also a strong down regulation of TEMT (thioether S-methyltransferase), an important enzyme involved in detoxification of selenium and sulfur containing compounds (47). An evolutionarily related gene for the enzyme nicotinamide N-methyltransferase (Nnmt), which methylates nicotinamide, is also regulated during starvation and sugar.

Cholesterol and DHEA regulation

DHEA is a cholesterol derived hormone which, together with its sulfated ester, DHEA-S, is present at the highest level of any circulating hormone in humans (1, 81). Our analysis reveals a striking regulatory pattern concerning DHEA metabolism (Fig 4; Table 7). First, genes involved in synthesis of cholesterol from acetyl CoA are down regulated (including the cytoplasmic form of HMG CoA synthase which produces HMG-CoA). Second, the key gene in DHEA biosynthesis from cholesterol, Cyp17a1 (steroid-17alpha-monooxygenase), is highly up regulated. Third, genes involved in converting DHEA to other compounds, such as bile acid and other steroids, are down regulated (Table 7). Fourth, there is a down regulation of Cyp7b1, which is involved in the breakdown of cholesterol to bile acid, and the corticosteroid binding globulin protein (CBG). In sum, the goal of these regulatory changes during fasting appears to be to maintain as high a level of DHEA as possible, both by increasing DHEA production from the available cholesterol pool and by decreasing DHEA conversion to other compounds.

As a side, we note that in contrast to the cytoplasmic form, the mitochondrial form of HMG CoA synthase is increased in starvation. The latter form is used in ketogenesis to make ketone bodies from acetyl CoA derived from fatty acid catabolism. This makes physiologic sense since ketone bodies provide fuel for the brain during starvation. It has further been reported that the mitochondrial HMG CoA synthase is directly regulated by forkhead transcription factor (FKHRL1) via the insulin signaling pathway (50).

IGFBP and IGF regulation

One of the most striking regulations is observed for insulin-like growth factor binding protein 1 (Igfbp1) (Figure 5, Table 8). It is unchanged at 24 hour starvation, but becomes highly up regulated after 48 hours. This up regulation is almost completely suppressed by sugar feeding. Igfbps function by binding insulin-like growth factors (Igfs), thereby interfering with Igf activity on target organs (35). Igfbp1 is the major form that controls body growth. Thus, it makes physiologic sense that starvation effects up regulation of Igfbp1, thereby signaling stoppage of cellular growth upon nutrient limitation. There is also a down regulation of Igf1, the cognate binding factor of Igfbp1. The results of other Igf/Igfbp members are shown in Table 8. The Igfbp1 signaling pathway is used not only during nutrient deprivation but in other processes that require stoppage of growth, including liver regeneration (67). This is probably because global body growth must be halted during the biosynthetic process of regenerating an organ. We have also seen a marked decrease in growth hormone (GH) gene expression in the brain upon starvation (unpublished data). This further reflects a coordinated alteration in growth factor signaling program (Figure 5).

DNA repair and apoptosis

In addition to changes in metabolic and hormonal systems in the face of nutrient shortage, animals must also stop growth since attempted proliferation in the absence of necessary biosynthetic resources would be detrimental to survival. Various genes which may

function to maintain genome integrity or coordinate cell proliferation and apoptosis are listed in Table 9. A highly up regulated gene is Gadd45b, which functions in growth arrest and is also inducible by DNA damage, genotoxic stress and TGF β signals (73, 82). As with Igfbp1, Gadd45s are also up regulated during liver regeneration (67). The LIM-only transcriptional regulator Lmo4 is implicated in proliferation control and is also up regulated (highest up regulated transcription factor in our microarray), as is the radiation-induced cysteine rich LIM protein gene Rad51L1 (61, 75). Other up regulated genes implicated in apoptosis include a Bcl-2 family member Bnip3 (5, 6, 53, 74), and Creg (cellular repressor of E1A suppressed genes), which encodes a glycoprotein involved in growth inhibition and binds to insulin-like growth factor receptor Igf2r (Table 8) (14). There is also strong down regulation SMP-30/regucalcin (Rgn), which has been implicated in calcium homeostasis and growth control (21, 49).

DISCUSSION

Connection between physiological pathways underlying starvation response and those regulating lifespan

In a large scale gene expression profile screen in mouse liver, we have identified several metabolic and signaling pathways whose components are altered transcriptionally in starved and sugar-fed conditions. Although the used microarray approach can not provide a direct link between changed RNA levels and influence on protein activity or metabolic

flux, we observe a strong correlation between these pathways and those which have been shown to be important for longevity. We outline below the similarities between starvation response and lifespan prolonging processes.

Lipid catabolism and activation of the oxidative stress response

The need for the body to break down lipids can come externally through dietary intake or internally through breakdown of endogenous lipids during fasting. We have observed large number of genes regulated upon starvation which are part of this lipid signaling cascade (9). The relevance for this cascade for aging is clear: it regulates a battery of anti-oxidant factors, including nuclear receptors and cytochrome P450s, for detoxification and protection from oxidative and xenobiotic stress. Since oxidative stress is one of the major sources thought to affect the aging process, factors that increase protection from oxidative stress should slow down aging. In *C. elegans* for example, the *daf9* and *daf12* genes, which affect lifespan, encode a cytochrome P450 and a nuclear receptor with similarity to PXR, respectively (3, 23). In *Drosophila*, it has recently been shown that the steroid hormone ecdysone, acting through its nuclear receptor, controls aging (62). Thus, the lipid activated nuclear receptor pathways would bring about increased resistance to oxidative stress, thereby increasing survival and longevity.

Regulation of central metabolic pathways: SAM and urea cycles

SAM, the central factor in methylation reactions in the cell, has long been implicated in cellular aging through regulation of various methyltransferases that participate in protein repair (10, 11, 64). It is interesting that the overall regulatory alterations in SAM cycle

upon starvation would have the effect of lowering homocysteine levels, since high homocysteine levels have been associated with increased chance for coronary diseases (19, 57). It has also been recently shown that in long-lived Ames dwarf mice the activities of *Mat1* and *Gnmt* are elevated (72); since both of these genes are up regulated upon starvation, it is consistent with the notion that increased flux through the SAM cycle is associated with lifespan extension and starvation response. Furthermore, the methyltransferase *Comt*, which is down regulated in starvation, has been implicated in Alzheimer's disease and its inhibitor is used to treat Parkinson's disease (78).

In contrast to the association of methyltransferase reactions with protein damage repair and aging, little has been documented on the potential role of urea cycle and aging. There is however one intriguing observation. It has recently been shown in *Drosophila* that feeding sodium 4-phenylbutyrate (PBA) can extend lifespan (32), and PBA is a FDA approved drug for treatment of urea cycle disorder (7). Another potential connection comes from a recent study showing that a gene involved in autophagy can extend lifespan in *C. elegans* (45). Since autophagy entails degradation of internal proteins in the face of nutrient deprivation, it will likely increase flux through the urea cycle.

Regulation of hormonal pathways: DHEA and insulin/Igf signaling

The level of DHEA and its sulfated derivative steadily decreases with age, a fact which underpins many discussions on its role as an anti-aging substance. The role of DHEA is controversial, but it has been implicated in a variety of processes associated with youth and virility (1, 44, 81). Our analysis indicates that upon starvation, the body tries to

maintain as high a level of DHEA as possible: the gene for DHEA synthesis from cholesterol is highly up regulated, whereas those which are involved in making other steroid hormones are down regulated. This further suggests a connection between starvation response and an anti-aging process.

There is substantial evidence for insulin/IGF signaling playing a fundamental role in aging. This comes from mammalian studies, as well as worms and flies (17, 36, 41). In these cases, decrease in insulin signaling is correlated with increased lifespan. Recent studies further suggest that insulin may increase the chance of Alzheimer's disease (70). Consistent with our view that starvation response shares signaling pathways with those underlying anti-aging processes, there is a large decrease in insulin signaling upon starvation as illustrated by the large increase in *Igfbp1* expression. The decreased insulin signaling could also affect cytochrome P450 activity through *Alas*, since it has been reported that insulin inhibits *Alas* in liver-derived cell line (56). Therefore, upon starvation decreased insulin level would de-repress expression of *Alas*, which is what is observed, leading to increased cytochrome P450 synthesis, thereby connecting the cytochrome P450 pathway with the insulin pathway.

Genome instability and apoptosis

Genes involved in maintaining genome integrity, such as DNA repair, play an important role in aging (31). The NAD dependent histone deacetylase *Sir2* in yeast and the histone acetylase *Rpd3* in *Drosophila* have been shown to regulate aging (39, 55). Furthermore,

yeast lifespan can be increased by changing the level of NAD through increased Nnmt (nicotinamide N-methyltransferase) activity (2), and we also see an increase in Nnmt upon starvation. It has also been suggested that certain compounds that extend lifespan in yeast through Sir2 operate by suppressing p53 and delaying apoptosis (27). In this respect, we note that Rad5111, which is up regulated in starvation, is a vital, radiation induced gene which may function through interaction with p53 (61). In addition, Starai et al (65) have pointed out a link between Sir2 function and lipid metabolism through the activation of acetyl CoA synthetase. Thus, many of the metabolic response to starvation may be mediated by factors that influence aging through their function in genome stability and cell survival.

Regulatory overlap between starvation response and caloric restriction

The one documented regimen for prolonging lifespan in various organisms has been caloric restriction (41, 63). Since starvation can be viewed as the most extreme form of caloric restriction, it is not surprising that many of the connections made here between starvation and longevity have been previously observed for caloric restriction and longevity. It is therefore also not surprising that lifespan extension is associated with increased survival under starvation stress in different organisms (40). Thus one can ask if the regulatory mechanisms that operate during starvation also operate during caloric restriction at the gene expression level. We indeed find informative overlaps between genes regulated for liver in caloric restricted mice and our current analysis. For example, carbamoyl phosphate synthetase of the urea cycle is up regulated upon starvation and

caloric restriction, whereas glutamine synthetase is down regulated in both cases (13, 71, 79). Furthermore, in a microarray analysis of calorically restricted mouse liver (8), 33 genes were identified as having caloric restriction specific changes. 28 of the genes are represented in our microarray, 19 out of these are regulated in the same direction, 5 in the opposite direction and 4 are unchanged. Of the 24 regulated ones, 9 can be found in the list of genes representing the signaling or metabolic pathways highlighted in our starvation condition, and 8 of the 9 genes are regulated in the same direction as in caloric restriction (Got1, Fasn, Gamt, Cypa13, Cyp4a14, Ese1, Cbg and Rgn; the one exception is Apoa4). Furthermore, the 8 genes are distributed over the different pathways and are not restricted to any specific one. This comparison reveals a significant overlap of the expression profile between starvation and caloric restricted conditions, although it should be emphasized that the comparison is based on a single study and further independent data will be required. On the other hand, while caloric restriction can extend lifespan, prolonged starvation is life threatening. What could then be the common theme linking starvation response to caloric restriction? We favor the view that it is the degree of response to stress brought upon by the two conditions. Caloric restriction might invoke a low level stress response which in the long run will have a protective function and increase survival; starvation would invoke a similar response but at a much higher level and which cannot be sustained for long periods. The genetic regulatory patterns that we have found in starvation could therefore lead to a better understanding of anti-aging mechanisms as well as global biological functions such as interactions between anti-oxidative reactions, xenobiotic protection and maintenance of genome integrity.

ACKNOWLEDGMENTS

We thank Simone Schindler, Andy Cato, Norma Howells, Kevin White, Martin Hofmann, Peter Herrlich and all members of the Pankratz lab for their help. This work was supported by the Forschungszentrum Karlsruhe and BMBF (Bundesministerium fuer Bildung und Forschung).

REFERENCES

1. Allolio B, and Arlt W. DHEA treatment: myth or reality? Trends in Endoc & Metab 13: 288-294, 2002.
2. Anderson RM, Bitterman KJ, Wood JG, Medvedik O, and Sinclair DA. Nicotinamide and PNC1 govern lifespan extension by caloric restriction in *Saccharomyces cerevisiae*. Nature 423: 181-185, 2003.
3. Antebi A, Yeh WH, Tait D, Hedgecock EM, and Riddle DL. daf-12 encodes a nuclear receptor that regulates dauer diapause and developmental age in *C. elegans*. Genes Dev 15: 1512-1527, 2000.
4. Bodnar JS, Chatterjee A, Castellani LW, Ross DA, Ohmen J, Cavalcoli J, Wu C, Dains KM, Catanese J, Chu M, Sheth SS, Charugundla D, Demant P, West DB, de Jong P, and Lusis AJ. Positional cloning of the combined hyperlipidemia gene Hyplip1. Nat Genet 30: 110-116, 2002.
5. Boyd JM, Malstrom S, Subramanian T, Venkatesh LK, Schaeper U, Elangovan B, D'Sa-Eipper C, and Chinnadurai G. Adenovirus E1B 19 kDa and Bcl-2 proteins interact with a common set of cellular proteins. Cell 79: 341-351, 1994.

6. Bruick RK. Expression of the gene encoding the proapoptotic Nip3 protein is induced by hypoxia. *Proc Natl Acad Sci* 97: 9082-9087, 2000.
7. Brusilow SW, Danney M, Waber LJ, Batshaw M, Buton B, Levitsky L, Roth K, McKeethren C, and Ward J. Treatment of episodic hyperammonemia in children with inborn errors of urea synthesis. *N Engl J Med* 310: 1630-1634, 1984.
8. Cao S, Dhabhi JM, Mote PL, and Spindler SR. Genomic profiling of short-and long-term caloric restriction effects in the liver of aging mice. *Proc Natl Acad Sci* 98: 10630-10635, 2001.
9. Chawla A, Repa JJ, Evans RM, and Mangelsdorf DJ. Nuclear receptors and lipid physiology: opening the X-files. *Science* 294: 1866-1870, 2001.
10. Clarke S. Protein methylation. *Curr Opin Cell Biol* 5: 977-983, 1993.
11. Clarke S. Aging as war between chemical and biochemical processes: protein methylation and the recognition of age-damaged proteins for repair. *Ageing Res Rev* 2: 263-285, 2003.
12. Danesch U, Hoeck W, and Ringold GM. Cloning and transcriptional regulation of a novel adipocyte-specific gene, Fsp27. CAAT-enhancer-binding protein (C/EBP) and

C/EBP-like proteins interact with sequences required for differentiation-dependent expression. *J Biol Chem* 267: 7185-7193, 1992.

13. Dhahbi JM, Mote PL, Wingo J, Tillman JB, Walford RL, and Spindler S. Calories and aging alter gene expression for gluconeogenic, glycolytic, and nitrogen-metabolizing enzymes. *Am J Physiol* 277: E352-E359, 2001.

14. Di Bacco A, and Gill G. The secreted glycoprotein CREG inhibits cell growth dependent on the mannose-6-phosphate/insulin-like growth factor II receptor. *Oncogene* 22: 5436-5445, 2003.

15. Figge A, Lammert F, Paigen B, Henkel A, Matern S, Korstanje R, Schneider BL, Chen F, Stoltenberg E, Spatz K, Hoda F, Cohen DE, and Green RM. Hepatic over-expression of murine *Abcb11* increases hepatobiliary lipid secretion and reduces hepatic steatosis. *J Biol Chem* (pub ahead of print), 2003.

16. Fijino T, Takei YA, Sone H, Ioka RX, Kamataki A, Magoori K, Takahashi S, Sakai J, Yamamoto TT. Molecular identification and characterization of two medium-chain acyl-CoA synthetases, MACS1 and the Sa gene product. *J Biol Chem* 276: 35961-35969, 2001.

17. Finch CE, and Ruvkun G. The genetics of aging. *Annu Rev Genomics Hum Genet* 2: 435-462, 2001.

18. FitzPatrick DR, Germain-Lee E, and Valle D. Isolation and characterization of rat and human cDNAs encoding a novel putative peroxisomal enoyl-CoA hydratase. *Genomics* 27: 457-466, 1995.
19. Ford ES, Smith SJ, Stroup DF, Steinberg KK, Mueller PW, and Thacker SB. Homocyst(e)ine and cardiovascular disease: a systematic review of the evidence with special emphasis on case-control studies and nested case-control studies. *Int J Epidemiol* 31: 59-70, 2002.
20. Forestier M, Banninger R, Reichen J, and Solioz M. Betaine homocysteine methyltransferase: gene cloning and expression analysis in rat liver cirrhosis. *Biochim Biophys Acta* 1638: 29-34, 2003.
21. Fujita T, Shirasawa T, and Maruyama N. Expression and structure of senescence marker protein-30 (SMP30) and its biological significance. *Mech Ageing Dev* 107: 271-280, 1999.
22. Gasmi L, and McLennan AG. The mouse *Nudt7* gene encodes a peroxisomal nudix hydrolase specific for coenzyme A and its derivatives. *Biochem J* 357: 33-38, 2001.

23. Gerisch B, Weitzel C, Kober-Eisermann C, Rottiers V, Antebi A. A hormonal signaling pathway influencing *C. elegans* metabolism, reproductive development, and life span. *Dev Cell* 1: 841-851, 2001.
24. Hertzel AV, and Bernlohr DA. Cloning and chromosomal location of the murine keratinocyte lipid-binding protein gene. *Gene* 221: 235-243, 1998.
25. Hill JO, Wyatt HR, Reed GW, and Peter JC. Obesity and the environment: where do we go from here? *Science* 299: 853-855, 2003.
26. Holla VR, Adas F, Imig JD, Zhao X, Price E, Olsen N, Kovacs WJ, Magnuson MA, Keeney DS, Breyer MD, Falck JR, Waterman MR, and Capdevila JH. Alterations in the regulation of androgen-sensitive Cyp4a monooxygenases cause hypertension. *Proc Natl Acad Sci* 98: 5211-5216, 2001.
27. Howitz KT, Bitterman KJ, Cohen HY, Lamming DW, Savu S, Wood JG, Zipkin RE, Chung P, Kisielewski A, Zhang L, Schere B, and Sinclair DA. Small molecule activators of sirtuins extend *Saccharomyces cerevisiae* lifespan. *Nature* 425: 191-196, 2003.
28. Hunt MC, Solaas K, Kase BF, and Alexson SE. Characterization of an acyl-CoA thioesterase that functions as a major regulator of peroxisomal lipid metabolism. *J Biol Chem* 277: 1128-1138, 2002.

29. Inubushi T, Shikiji M, Endo K, Kakegawa H, Kishino Y, Katunuma N. Hormonal and dietary regulation of lysosomal cysteine proteinases in liver under gluconeogenesis conditions. *Biol Chem* 377: 539-542, 1996.
30. Jogl G, and Tong L. Crystal structure of carnitine acetyltransferase and implications for the catalytic mechanism and fatty acid transport. *Cell* 112: 113-122, 2003.
31. Johnson FB, Sinclair, DA, and Guarente L. Molecular biology of aging. *Cell* 96: 291-302, 1999.
32. Kang H, Benzer S, and Min K. Life extension in *Drosophila* by feeding a drug. *Proc Natl Acad Sci* 99: 838-843, 2002.
33. Kappas A, Sassa S, Galbraith RA, and Nordmann Y. The porphyrias. In: *The metabolic basis of inherited disease*, edited by Scriver CR, Beaudet AL, Sly WS, Valle D: McGraw Hill, 1989.
34. Karlic H, Leohninger A, Laschan C, Lapin A, Bohmer F, Huemer M, Guthann E, Rappold E, and Pfeilstocker M. Downregulation of carnitine acetyltransferases and organic cation transporter OCTN2 in mononuclear cells in healthy elderly and patients with myelodysplastic syndromes. *J Mol Med* 81: 435-442, 2003.

-
35. Kelley KM, Oh Y, Gargosky SE, Gucev Z, Matsumoto T, Hwa V, Ng L, Simpson DM, and Rosenfeld RG. Insulin-like growth factor-binding proteins (IGFBPs) and their regulatory dynamics. *Int J Biochem Cell Biol* 28: 619-637, 1996.
36. Kenyon C. A conserved regulatory systems for aging. *Cell* 105: 165-168, 2001.
37. Kikuta Y, Kasyu H, Kusunose E, and Kusunose M. Expression and catalytic activity of mouse leukotriene B4 omega-hydroxylase, CYP4F14. *Arch Biochem Biophys* 383: 225-232, 2000.
38. Kurtz DM, Tolwani RJ, and Wood PA. Structural characterization of the mouse long-chain acyl-CoA dehydrogenase gene and 5' regulatory region. *Mamm Genome* 9: 361-365, 1998.
39. Lin SJ, Defossez PA, and Guarente L. Requirement of NAD and SIR2 for life-span extension by calorie restriction in *Saccharomyces cerevisiae*. *Science* 289; 2022-2068, 2000.
40. Longo, VD. Mutations in signal transduction proteins increase stress resistance and longevity in yeast, nematodes, fruit flies, and mammalian neuronal cells. *Neurobiol aging* 20: 479-486, 1999.

41. Longo VD, and Finch CE. Evolutionary medicine: from dwarf model systems to healthy centenarians? *Science* 299: 1342-1346, 2003.
42. Lu SC, Alvarez L, Huang ZZ, Chen L, An W, Corrales FJ, Avila MA, Kanel G, and Mato JM. Methionine adenosyltransferase 1A knockout mice are predisposed to liver injury and exhibit increased expression of genes involved in proliferation. *Proc Natl Acad Sci* 98: 5560-5565, 2001.
43. Mato JM, Corrales FJ, Lu SC, Avila MA. S-adenosylmethionine: a control switch that regulates liver function. *FASEB J* 16: 15-26, 2002.
44. Mazat L, Lafont S, Berr C, Debuire B, Tessier JF, Dartigues JF, and Baulieu EE. Prospective measurements of dehydroepiandrosterone sulfate in a cohort of elderly subjects: relationship to gender, subjective health, smoking habits, and 10-year mortality. *Proc Natl Acad Sci* 98: 8145-8150, 2001.
45. Melendez A, Tallochy Z, Seaman M, Eskelinen E, Hall DH, and Levine B. Autophagy genes are essential for dauer development and life-span extension in *C. elegans*. *Science* 301: 1387-1391, 2003.
46. Michal M. *Biochemical Pathways*. Heidelberg: Akademische Verlag, 1999.

-
47. Mozier NM, McConnell KP, Hoffman JL. S-adenosyl-L-methionine: thioether-S-methyltransferase, a new enzyme in sulfur and selenium metabolism. *J Biol Chem* 263: 4527-4531. 1988.
48. Muoio DM, and Lynis Dohm G. Peripheral metabolic actions of leptin. *Best Pract Res Clin Endocrinol Metab* 16: 653-666, 2002.
49. Murata T, and Yamaguchi M. Molecular cloning of the cDNA coding for regucalcin and its mRNA expression in mouse liver: the expression is stimulated by calcium administration. *Mol Cell Biochem* 173: 127-133, 1997.
50. Nadal A, Marrero PF, and Haro D. Down-regulation of the mitochondrial 3-hydroxy-3-methylglutaryl-coA synthase gene by insulin: the role of the forkhead transcription factor FKHRL1. *Biochem J* 366: 289-297, 2002.
51. Ntambi JM, Miyazaki M, Stoehr JP, Lan H., Kendzioriski CM, Yandell BS, Song Y, Cohen, P, Friedman J, Attie AD. Loss of stearoyl-CoA desaturase-1 function protects mice against adiposity. *Proc Natl Acad Sci* 99: 11482-11486, 2002.
52. Ntambi JM, and Miyazaki M. Recent insights into stearoyl-CoA desaturase-1. *Curr Opin Lipidol* 14: 255-261, 2003.

53. Ray R, Chen G, Vande C, Cizeau J, Park JH, Reed Jc, Gietz RD, Greenberg AH. BNIP3 heterodimerizes with Bcl-2/Bcl-X(L) and induces cell death independent of a Bcl-2 homology 3 (BH3) domain at both mitochondrial and nonmitochondrial sites. *J Biol Chem* 275: 1439-1448, 2000.
54. Ren S, Marques D, Redford K, Hylemon PB, Gil G, Vlahcevic ZR, Pandak WM. Regulation of oxysterol 7 α -hydroxylase (CYP7B1) in the rat. *Metabolism* 52: 636-642, 2003.
55. Rogina B., Helfand S, and Frankel S. Longevity regulation by *Drosophila* Rpd3 deacetylase and caloric restriction. *Science* 298: 1745, 2002.
56. Scassa M, Varone C, Montero L, Canepa ET. Insulin inhibits delta-aminolevulinate synthase gene expression in rat hepatocytes and human hepatoma cells. *Exp Cell Res* 244: 460-469, 1998.
57. Schaefer EJ. Lipoproteins, nutrition, and heart disease. *Am J Clin Nutr* 75: 191-212, 2002.
58. Scislawski PW, Foster AR, and Fuller MF. Regulation of oxidative degradation of L-lysine in rat liver mitochondria. *Biochem J* 300: 887-891, 1994.

59. Scriver CR, Beaudet L, Sly WS, and Valle D. The metabolic basis of inherited disease. New York: McGraw Hill, 1989.

60. Shalev A, Pise-Masison CA, Radonovich M, Hoffmann SC, Hirschberg B, Brady JN, and Harlan DM. Oligonucleotide microarray analysis of intact human pancreatic islets: identification of glucose-responsive genes and a highly regulated TGF β signaling pathway. *Endocrinology* 142: 3695-3698, 2002.

61. Shu Z, Smith S, Wang L, Rice MC, and Kmiec EB. Disruption of muREC2/RAD51L1 mice results in early embryonic lethality which can be partially rescued in a p53(-/-) background. *Mol Cell Biol* 12: 8686-8693, 1999.

62. Simon AF, Shih C, Mack A, and Benzer S. Steroid control of longevity in *Drosophila melanogaster*. *Science* 299: 1407-1410, 2003.

63. Sohal RS and Weindruch R. Oxidative stress, caloric restriction, and aging. *Science* 273: 59-63, 1996.

64. Stadman ER. Protein oxidation and aging. *Science* 257: 1220-1224, 1992.

65. Starai VJ, Celic I, Cole RN, Boeke JD, and Escalante-Semerena JC. Sir2-dependent activation of acetyl-CoA synthetase by deacetylation of active lysine. *Science* 298: 2390-2392, 2002.

-
66. Stypmann J, Gläser K, Roth W, Tobin DJ, Petermann I, Matthias R, Mönnig G, Haverkamp W, Breithardt G, Schmahl W, Peters C, and Reinheckel T. Dilated cardiomyopathy in mice deficient for the lysosomal cysteine peptidase cathepsin L. *Proc Natl Acad Sci* 99: 6234-6239, 2002.
67. Su AI, Guidotti LG, Pezacki JP, Chisari F, and Schultz PG. Gene expression during the priming phase of liver regeneration after partial hepatectomy in mice. *Proc Natl Acad Sci* 99: 11181-11186, 2002.
68. Tatar M, Bartke A, and Antebi A. The endocrine regulation of aging by insulin-like signals. *Science* 299: 1346-1351, 2003.
69. Taubes G. The soft science of dietary fat. *Science* 29: 2536-2545, 2001.
70. Taubes G. Insulin insults may spur Alzheimer's disease. *Science* 301: 40-41, 2003.
71. Tillman JB, Dhahbi JM, Mote PL, Walford RL, and Spindler SR. Dietary caloric restriction in mice induces carbamyl phosphate synthetase I gene transcription tissue specifically. *J Biol Chem* 271: 3500-3506, 1996.
72. Uthus EO, and Brown-Borg HM. Altered methionine metabolism in long living Ames dwarf mice. *Exp Gerontol* 38: 491-498, 2002.

73. Vairapandi M, Balliet AG, Hoffman B, and Liebermann DA. GADD45b and GADD45g are cdc2/cyclinB1 kinase inhibitors with a role in S and G2/M cell cycle checkpoints induced by genotoxic stress. *J Cell Physiol*. 192: 327-338, 2002.
74. Vande Velde C, Cizeau J, Dubik D, Alimonti J, Brown T, Israels S, Hakem R, and Greenberg AH. BNIP3 and genetic control of necrosis-like cell death through the mitochondrial permeability transition pore. *Mol Cell Biol* 15: 5454-5468.
75. Visvader JE, Venter D, Hahm K, Santamaria M, Sum EY, O'Reilly L, White D, Williams R, Armes J, and Lindeman GJ. The LIM domain gene LMO4 inhibits differentiation of mammary epithelial cells in vitro and is overexpressed in breast cancer. *Proc Natl Acad Sci* 98: 14452-14457, 2001.
76. Wang Y, De Keulenaer GW, and Lee RT. Vitamin D(3)-up-regulated protein-1 is a stress-responsive gene that regulates cardiomyocyte viability through interaction with thioredoxin. *J Biol Chem* 277: 26496-26500, 2002.
77. Watanabe R, Fujii H, Odani S, Sakakibara J, Yamamoto A, Ito M, Ono T. Molecular cloning of a cDNA encoding a novel fatty acid-binding protein from rat skin. *Biochem Biophys Res Commun* 200: 253-259, 1994.

78. Waters C. Practical issues with COMT inhibitors in Parkinson's disease. *Neurology* 55: S57-S59, 2000.
79. Weindruch R, Kayo T, Lee CK, and Prolla TA. Microarray profiling of gene expression in aging and its alteration by caloric restriction in mice. *J Nutr* 131: 918S-923S, 2001.
80. Yang YH, Dudoit S, Luu P, Lin DM, Peng V, Ngai J, and Speed TP. Normalization for cDNA microarray data: robust composite method addressing single and multiple slide systematic variation. *Nucleic Acids Res.* 30: e15, 2002.
81. Yen S. Dehydroepiandrosterone sulfate and longevity: new clues for an old friend. *Proc Natl Acad Sci* 98: 8167-8169, 2001.
82. Yoo J, Ghiassi M, Jirmanova L, Balliet AG, Hoffman B, Fornace AJ, Liebermann DA, Bottinger EP, and Roberts AB. Transforming growth factor-beta-induced apoptosis is mediated by Smad-dependent expression of GADD45b through p38 activation. *J Biol Chem* 278: 43001-43007, 2003.
83. Zhao XQ, Latinwo L, Liu XX, Lee ES, Lamango N, and Charlton CG. L-dopa upregulates the expression and activities of methionine adenosyl transferase and catechol-O-methyltransferase. *Exp Neurol* 171: 127-138, 2001.

-
84. Zimmet P, Alberti K, and Shaw J. Global and societal implications of the diabetes epidemic. *Nature* 414: 782-787, 2001.
85. Zinke I, Schütz CS, Katzenberger JD, Bauer M, and Pankratz, MJ. Nutrient control of gene expression in *Drosophila*: microarray analysis of starvation and sugar-dependent response. *EMBO J* 22: 6162-6173, 2002.
86. Zubieta J, Heitzeg MM, Smith YR, Bueller JA, Xu K, Xu Y, Koeppe RA, Stohler CS, and Goldman D. COMT val158met genotype affects u-opioid neurotransmitter responses to a pain stressor. *Science* 299: 1240-1243, 2003.

FIGURE LEGENDS**Figure 1**

Number and overlap of more than two fold regulated genes between the three nutrient conditions

Figure 2

The urea cycle and its connection to aspartate cycle. The + and – signs on red colored arrows designate up or down regulation, respectively, in the expression of genes encoding the enzymes shown. The numbers refer to the numbers in Table 5. Dashed arrows indicate summarized reactions. Metabolites are displayed in ellipses, enzymes in rectangles.

Figure 3

The S-adenosylmethionine (SAM) cycle. The numbers refer to the numbers in Table 6. The other markings are as in Figure 2. Numbers on black arrows designate not regulated enzymes.

Figure 4

Cholesterol and DHEA metabolism. The numbers refer to the numbers in Table 7. The other markings are as in Figure 2.

Figure 5

Insulin and IGF1 actions. Genes are displayed in ellipses with white background. The numbers refer to the numbers in Table 8, arrows extending from the genes denote their transcription pattern. Proteins are shown as rectangular shapes and written in capitalized letters. Arrows indicate positive influence; blunt-ended lines indicate negative influence. The red arrows denote predicted increase (arrow upwards) or decrease (arrow downwards) of the given components.

TABLESTable 1. *Experimental overview*

| feeding regime | treated group | control group | micro-arrays | dye swap |
|----------------|---------------|---------------|--------------|----------|
| 24h starvation | 6 | 6 | 24 | 12/12 |
| 48h starvation | 10 | 10 | 24 | 12/12 |
| 48h high sugar | 10 | 10 | 12 | 7/5 |

In the column “dye swap” the number of microarrays hybridized in each dye swap direction is listed. As each array contains two subarrays, the maximum number of data points per gene is double the number of used microarrays.

Table 2. Selected enzymes and regulatory proteins of fatty acid and lipid metabolism

| # | enzyme | gene symbol | 24h starved | 48h starved | 48h sugar |
|-----------------------|--|-------------|-------------|-------------|-----------|
| <i>up regulated</i> | | | | | |
| 1 | peroxisomal acyl-CoA thioesterase 2A | Pte2a | +6.30 | +8.89 | +3.62 |
| 2 | apolipoprotein A-IV | Apoa4 | +4.77 | +5.50 | +3.14 |
| 3 | fat specific gene 27 | Fsp27 | +1.37 | +4.00 | n |
| 4 | leptin receptor | Lepr | +1.23 | +3.84 | +1.38 |
| 5 | thioredoxin interacting protein | Txnip | n | +3.52 | +1.70 |
| 6 | carnitine acetyltransferase | Crat | +2.63 | +3.52 | +2.34 |
| 7 | adipose differentiation related protein | Adfp | +2.26 | +3.18 | +1.67 |
| 8 | similar to bile acid Coenzyme A (<i>M. musculus</i>), amino acid N-acetyltransferase (glycine N-choloyl-transferase) | AK050308 | +2.14 | +3.02 | +1.32 |
| 9 | enoyl Coenzyme A hydratase 1, peroxisomal | Ech1 | +2.17 | +2.53 | +1.37 |
| 10 | acetyl-Coenzyme A acyltransferase 1, peroxisomal 3-ketoacyl-CoA thiolase (Ptl) | Acaa1 | +2.53 | +2.23 | +1.29 |
| 11 | acetyl-Coenzyme A dehydrogenase, long-chain | Acadl | +1.89 | +2.12 | +1.41 |
| <i>down regulated</i> | | | | | |
| 12 | unknown, contains apoL domain, similar to apolipoprotein 2 (<i>R. norvegicus</i>) | BC020489 | -1.78 | -7.48 | n |
| 13 | stearoyl-Coenzyme A desaturase 1 | Scd1 | -3.88 | -5.01 | +3.19 |
| 14 | esterase 31 | Es31 | -2.00 | -4.06 | -1.45 |
| 15 | nudix (nucleoside diphosphate linked moiety X)-type motif 7 | Nudt7 | -5.10 | -3.99 | -2.10 |
| 16 | serum amyloid A 1 | Saa1 | -1.63 | -3.64 | n |
| 17 | esterase 1 | Es1 | -1.45 | -3.41 | n |
| 18 | serum amyloid A 4 | Saa4 | -2.18 | -3.40 | -1.51 |
| 19 | similar to carboxylesterase precursor (<i>M. auratus</i>) | AK078953 | -1.85 | -3.35 | n |
| 20 | similar to liver carboxylesterase 4 (<i>R. norvegicus</i>) | BC013479 | -1.49 | -2.73 | n |
| 21 | butyryl Coenzyme A synthetase 1 | Bucs1 | -2.24 | -2.69 | -1.32 |
| 22 | similar to carboxylesterase 2 (<i>M. musculus</i>) | BC024548 | -1.61 | -2.50 | n |
| 23 | esterase 22 | Es22 | -1.44 | -2.30 | -1.16 |
| 24 | serum amyloid A 3 | Saa3 | +1.13 | -1.87 | n |
| 25 | fatty acid synthase | Fasn | -2.07 | -1.57 | +2.57 |

In cases where no gene symbol is known in literature, it is replaced by the NCBI Genebank accession number. In the columns “24h starved”, “48h starved” and “48h sugar” the relative fold change of the starved and sugar fed

animals compared with the normal fed control is listed. “n” indicates no significant change. The genes are ordered according to the “48h starved” values, descending for the up regulated and ascending for the down regulated genes.

Table 3. *Nuclear receptors, fatty acid binding proteins and ABC transporters*

| # | gene | gene symbol | 24h starved | 48h starved | 48h sugar |
|--|---|-------------|-------------|-------------|-----------|
| <i>nuclear receptors</i> | | | | | |
| 1 | nuclear receptor subfamily 1, group I, member 2, pregnane X receptor (Pxr) | Nr1i2 | +1.23 | +1.83 | +1.34 |
| 2 | nuclear receptor subfamily 1, group I, member 3, constitutive androstane receptor (Car) | Nr1i3 | +2.21 | +1.76 | +1.36 |
| 3 | retinoid X receptor alpha | Rxra | n | -1.07 | n |
| 4 | peroxisome proliferator activator receptor alpha | Ppara | n | n | +1.15 |
| 5 | peroxisome proliferator activator receptor delta | Ppard | n | n | n |
| 6 | retinoid X receptor beta | Rxrb | +1.14 | n | n |
| 7 | retinoid X receptor gamma | Rxrg | n | n | n |
| 8 | vitamin D receptor | Vdr | n | n | n |
| <i>fatty acid binding proteins</i> | | | | | |
| 9 | muscle and heart specific (H-Fabp) | Fabp3 | n | n | n |
| 10 | ileal lipid binding | Fabp6 | n | n | n |
| 11 | adipocyte specific | Fabp4 | -1.15 | -1.42 | n |
| 12 | liver specific (L-Fabp) | Fabp1 | -1.51 | -2.29 | -1.41 |
| 13 | epidermal specific (E-Fabp), keratinocyte lipid binding protein | Fabp5 | -9.18 | -14.26 | -1.75 |
| <i>ABC (ATP-binding cassette) transporters</i> | | | | | |
| 14 | sub-family D (Ald), member 3 | Abcd3 | +1.42 | +1.48 | +1.30 |
| 15 | sub-family B (Mdr/Tap), member 4 | Abcb4 | +1.39 | +1.47 | 1.19 |
| 16 | sub-family C (Cftr/Mrp), member 3 | Abcc3 | +1.53 | +1.25 | |
| 17 | sub-family D (Ald), member 1 | Abcd1 | n | +1.23 | +1.10 |
| 18 | sub-family A (Abc1), member 6 | Abca6 | +1.43 | +1.21 | n |
| 19 | sub-family C (Cftr/Mrp), member 1 | Abcc1 | +1.32 | n | n |
| 20 | sub-family E (Oabp), member 1 | Abce1 | -1.09 | n | n |
| 21 | sub-family F (Gcn20), member 3 | Abcf3 | -1.18 | n | n |
| 22 | sub-family F (Gcn20), member 2 | Abcf2 | n | n | +1.10 |
| 23 | sub-family A (Abc1), member 2 | Abca2 | n | -1.12 | n |
| 24 | transporter 1, sub-family B (Mdr/Tap) | Tap1 | n | -1.20 | n |
| 25 | sub-family B (Mdr/Tap), member 10 | Abcb10 | -1.79 | -1.67 | n |
| 26 | sub-family B (Mdr/Tap), member 11 | Abcb11 | -2.19 | -3.47 | -1.39 |

In this table all nuclear receptors and fatty acid binding proteins which function in the context of the Cytochrome P450 regulation and are represented on the microarrays are listed. Additionally all regulated ABC transporters are

given. In the columns “24h starved”, “48h starved” and “48h sugar” the relative fold change of the starved and sugar fed animals compared with the normal fed control is listed. “n” indicates no significant change. The genes are ordered descending according to the “48h starved” values.

Table 4. *Cytochrome P450s and aminolevulinic acid synthases*

| # | cytochrome P450 | gene symbol | 24h starved | 48h starved | 48h sugar |
|--------------------------------------|--|-------------|-------------|-------------|-----------|
| <i>cytochrome P450s</i> | | | | | |
| 1 | family 4, subfamily a, polypeptide 14 | Cyp4a14 | +47.39 | +50.07 | +4.49 |
| 2 | family 17, subfamily a, polypeptide 1 | Cyp17a1 | +3.17 | +6.28 | n |
| 3 | family 2, subfamily a, polypeptide 5 | Cyp2a5 | +1.84 | +2.18 | n |
| 4 | family 2, subfamily b, polypeptide 20 | Cyp2b20 | n | +1.62 | n |
| 5 | family 3, subfamily a, polypeptide 13 | Cyp3a13 | +1.69 | +1.54 | +1.37 |
| 6 | family 3, subfamily a, polypeptide 11 | Cyp3a11 | +1.53 | +1.34 | +1.31 |
| 7 | family 2, subfamily a, polypeptide 12 | Cyp2a12 | n | +1.31 | n |
| 8 | family 2, subfamily d, polypeptide 2 | Cyp2d2 | +1.31 | +1.12 | n |
| 9 | family 11, subfamily a, polypeptide 1 | Cyp11a1 | n | -1.07 | n |
| 10 | family 2, subfamily d, polypeptide 26 | Cyp2d26 | +1.14 | -1.15 | +1.27 |
| 11 | family 2, subfamily d, polypeptide 22 | Cyp2d22 | n | -1.18 | n |
| 12 | family 4, subfamily b, polypeptide 1 | Cyp4b1 | +1.15 | -1.18 | n |
| 13 | family 27, subfamily a, polypeptide 1 | Cyp27a1 | n | -1.29 | -1.91 |
| 14 | family 2, subfamily d, polypeptide 3 | Cyp2d3 | n | -1.38 | +1.18 |
| 15 | family 2, subfamily j, polypeptide 9 | Cyp2j9 | -1.30 | -1.45 | n |
| 16 | family 4, subfamily f, polypeptide 13 | Cyp4f13 | -1.46 | -1.46 | -1.44 |
| 17 | family 4, subfamily f, polypeptide 3 | Cyp4f3 | -1.48 | -1.51 | -1.32 |
| 18 | family 4, subfamily f, polypeptide 16 | Cyp4f16 | -1.47 | -1.56 | n |
| 19 | family 2, subfamily f, polypeptide 2 | Cyp2f2 | -1.39 | -2.33 | -1.57 |
| 20 | family 4, subfamily v, polypeptide 3 | Cyp4v3 | -1.75 | -2.77 | -1.37 |
| 21 | family 7, subfamily b, polypeptide 1 | Cyp7b1 | -3.70 | -6.28 | -2.45 |
| 22 | family 4, subfamily f, polypeptide 14 | Cyp4f14 | -5.02 | -7.26 | -1.71 |
| 23 | family 2, subfamily c, polypeptide 70 | Cyp2c70 | -18.54 | -24.78 | -3.38 |
| <i>aminolevulinic acid synthases</i> | | | | | |
| 24 | aminolevulinic acid synthase 1, glycine C-succinyl transferase | Alas1 | n | +1.98 | n |
| 25 | aminolevulinic acid synthase 2 (erythroid-specific) | Alas2 | -1.55 | -2.39 | -1.56 |

In this table all regulated cytochrome P450s and aminolevulinic acid synthase 1 and 2, represented on the micro-arrays are listed. In the columns “24h starved”, “48h starved” and “48h sugar” the relative fold change of the starved and sugar fed animals compared with the normal fed control is listed. “n” indicates no significant change. The genes are ordered descending according to the “48h starved” values.

Table 5. *Regulated enzymes of urea cycle and selected enzymes of amino acid metabolism*

| # | enzyme | gene symbol | 24h starved | 48h starved | 48h sugar |
|------------------------------|---|-------------|-------------|-------------|-----------|
| <i>urea cycle</i> | | | | | |
| 1 | aspartate aminotransferase (cytosolic) | Got1 | +2.28 | +6.08 | -1.77 |
| 2 | argininosuccinate lyase | Asl | +2.61 | +4.07 | -1.21 |
| 3 | arginase (liver type) | Arg1 | +2.13 | +3.18 | -1.38 |
| 4 | carbamoyl phosphate synthetase | AK028683 | +1.25 | +2.17 | -1.87 |
| <i>amino acid metabolism</i> | | | | | |
| 5 | cathepsin L | Ctsl | n | +4.71 | n |
| 6 | aminoadipate-semialdehyde synthase, lysine oxoglutarate reductase, saccharopine dehydrogenase | Aass | +1.34 | +2.96 | +1.57 |
| 7 | glutamate-ammonia ligase, glutamine synthetase | Glul | -1.86 | -2.90 | -2.47 |
| 8 | carbonic anhydrase 1 | Car1 | -2.33 | -2.01 | -1.44 |
| 9 | carbonic anhydrase 3 | Car3 | -16.83 | -57.51 | -1.96 |

Numbers used in figure 2 are found in the first column. In cases where no gene symbol is known in literature, it is replaced by the NCBI Genebank accession number. In the columns “24h starved”, “48h starved” and “48h sugar” the relative fold change of the starved and sugar fed animals compared with the normal fed control is listed. “n” indicates no significant change. The genes are ordered descending according to the “48h starved” values.

Table 6. *Regulated enzymes of the SAM cycle, subsequent reactions and methyl transferases*

| # | enzyme | gene symbol | 24h starved | 48h starved | 48h sugar |
|---|--|-------------|-------------|-------------|-----------|
| <i>SAM cycle and subsequent reactions</i> | | | | | |
| 1 | methionine adenosyltransferase | Mat1a | +3.51 | +5.78 | +1.38 |
| 2 | betaine-homocysteine methyltransferase | Bhmt | +2.99 | +3.02 | -4.10 |
| 3 | glycine N-methyltransferase | Gnmt | +1.14 | +1.36 | -2.21 |
| 4 | adenosylhomocysteinase | BC051504 | n | n | n |
| 5 | dimethylglycine dehydrogenase | AK004755 | +1.13 | n | -1.18 |
| <i>methyl transferases</i> | | | | | |
| 6 | nicotinamide N-methyltransferase | Nnmt | +1.54 | +1.56 | -1.54 |
| 7 | guanidinoacetate methyltransferase | Gamt | -1.92 | -2.60 | n |
| 8 | catechol-O-methyltransferase | Comt | -2.33 | -5.18 | n |
| 9 | thioether S-methyltransferase | Temt | -5.62 | -8.04 | -1.48 |

Numbers used in figure 3 are found in the first column. In cases where no gene symbol is known in literature, it is replaced by the *NCBI Genebank* accession number. In the columns “24h starved”, “48h starved” and “48h sugar” the relative fold change of the starved and sugar fed animals compared with the normal fed control is listed. “n” indicates no significant change. The genes are ordered descending according to the “48h starved” values.

Table 7. *Regulated enzymes of cholesterol and DHEA metabolism*

| # | enzyme | gene symbol | 24h starved | 48h starved | 48h sugar |
|---|---|-------------|-------------|-------------|-----------|
| <i>cholesterol and DHEA metabolism</i> | | | | | |
| 1 | isopentenyl-diphosphate delta isomerase | Idi1 | -7.92 | -3.96 | -3.44 |
| 2 | farnesyl diphosphate synthetase | Fdps | -2.69 | -2.18 | -1.65 |
| 3 | squalene epoxidase | Sqle | -4.29 | -2.43 | -1.81 |
| 4 | sterol-C5-desaturase, lathosterol oxidase | Sc5d | -3.00 | -1.89 | -1.94 |
| 5 | cytochrome P450 family 17, subfamily a, polypeptide 1, steroid-17 α -monooxygenase | Cyp17a1 | +3.17 | +6.28 | n |
| 6 | steroid- Δ -isomerase: hydroxysteroid dehydrogenase-2, delta ⁵ -3-beta | Hsd3b2 | -4.55 | -5.16 | -1.64 |
| 6 | steroid- Δ -isomerase: hydroxysteroid dehydrogenase-3, delta ⁵ -3-beta | Hsd3b3 | -4.76 | -8.05 | -1.79 |
| 6 | steroid- Δ -isomerase: hydroxysteroid dehydrogenase-4, delta ⁵ -3-beta | Hsd3b4 | -6.44 | -3.96 | -1.53 |
| 7 | hydroxysteroid (17-beta) dehydrogenase 2, estradiol-17beta-dehydrogenase 2 | Hsd17b2 | -1.95 | -2.22 | -1.58 |
| 8 | serine (or cysteine) proteinase inhibitor, clade A, member 6, corticosteroid binding globulin (Cbg) | Serpina6 | -2.56 | -8.04 | +1.32 |
| 9 | family 7, subfamily b, polypeptide 1 | Cyp7b1 | -3.70 | -6.28 | -2.45 |
| <i>hydroxy-methylglutaryl-CoA synthases</i> | | | | | |
| 10 | 3-hydroxy-3-methylglutaryl-Coenzyme A synthase 1 (cytoplasmic) | Hmgcs1 | -3.56 | -2.98 | -2.57 |
| 11 | 3-hydroxy-3-methylglutaryl-Coenzyme A synthase 2 (mitochondrial) | Hmgcs2 | +2.59 | +2.67 | +1.45 |

Numbers used in figure 4 are found in the first column. In the columns “24h starved”, “48h starved” and “48h sugar” the relative fold change of the starved and sugar fed animals compared with the normal fed control is listed.

“n” indicates no significant change.

Table 8. *Insulin like growth factors and their regulatory proteins*

| # | gene | gene symbol | 24h starved | 48h starved | 48h sugar |
|---|---|-------------|--------------|-------------|-----------|
| <i>Igf binding and complexed proteins</i> | | | | | |
| 1 | insulin-like growth factor binding protein 1 | Igfbp1 | n | +25.91 | +1.38 |
| 2 | insulin-like growth factor binding protein 2 | Igfbp2 | +2.76 | +2.85 | -1.42 |
| 3 | insulin-like growth factor binding protein 3 | Igfbp3 | -1.26 | -1.11 | -1.16 |
| 4 | insulin-like growth factor binding protein 4 | Igfbp4 | n | -1.22 | -1.19 |
| 5 | insulin-like growth factor binding protein 6 | Igfbp6 | n | n | n |
| 6 | cysteine rich protein 61 (Igfbp10) | Cyr61 | +1.15 | n | +1.14 |
| 7 | insulin-like growth factor 2, binding protein 1 | Igf2bp1 | n | n | n |
| 8 | insulin-like growth factor 2, binding protein 3 | Igf2bp3 | n | n | n |
| 9 | insulin-like growth factor 2, binding protein 3 | Igf2bp3 | n | +1.06 | n |
| 10 | insulin-like growth factor binding protein, acid labile subunit | Igfals | n | -1.83 | -1.15 |
| <i>insulin like growth factors (Igf)</i> | | | | | |
| 11 | insulin-like growth factor 1 | Igf1 | -1.56 | -2.05 | -1.74 |
| 12 | insulin-like growth factor 2 | Igf2 | n | +1.23 | n |
| 13 | insulin-like 6 | Insl6 | n | +1.14 | n |
| <i>Igf receptors</i> | | | | | |
| 14 | insulin-like growth factor 1 receptor | Igf1r | not included | | |
| 15 | insulin-like growth factor 2 receptor | Igf2r | n | -1.04 | n |

In this table all insulin like growth factors and the regulatory proteins which are represented on the microarrays are listed. For the sake of completeness Igf1r is also mentioned. Numbers used in figure 5 are found in the first column. In the columns “24h starved”, “48h starved” and “48h sugar” the relative fold change of the starved and sugar fed animals compared with the normal fed control is listed. “n” indicates no significant change.

Table 9. *DNA repair and apoptosis genes*

| # | gene | gene symbol | 24h starved | 48h starved | 48h sugar |
|---|--|-------------|-------------|-------------|-----------|
| 1 | growth arrest and DNA-damage-inducible 45 beta | Gadd45b | +2.27 | +4.61 | n |
| 2 | LIM domain only 4 | Lmo4 | +1.52 | +3.77 | n |
| 3 | programmed cell death 5, TF-1 cell apoptosis related gene 19 protein (Tfar 19) | Pdcd5 | +1.61 | +3.59 | n |
| 4 | Rad51-like 1 | Rad5111 | +3.75 | +3.20 | +1.69 |
| 5 | Bcl2/adenovirus E1b 19kDa-interacting protein 1, Nip3 | Bnip3 | +2.05 | +2.90 | +1.15 |
| 6 | CCAAT/enhancer binding protein (C/EBP), delta | Cebpd | +1.45 | +2.39 | n |
| 7 | Jun oncogene | Jun | +1.35 | +2.29 | n |
| 8 | cellular repressor of E1A-stimulated genes | Creg | +1.66 | +2.15 | +1.33 |
| 9 | regucalcin, senescence marker protein 30 (Smp 30) | Rgn | -3.21 | -6.20 | -1.40 |

In the columns “24h starved”, “48h starved” and “48h sugar” the relative fold change of the starved and sugar fed animals compared with the normal fed control is listed. “n” indicates no significant change. The genes are ordered descending according to the “48h starved” values.

FIGURES

Figure 1

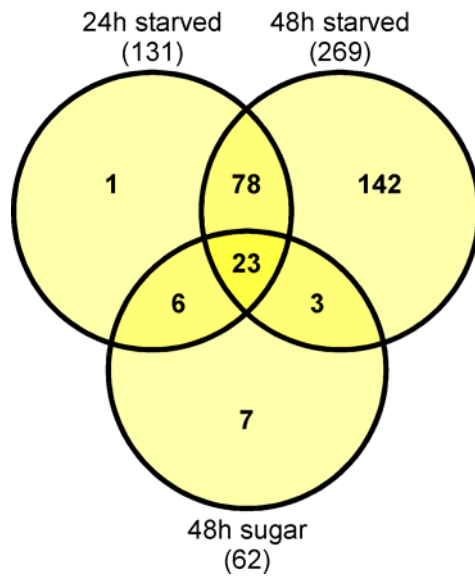


Figure 2

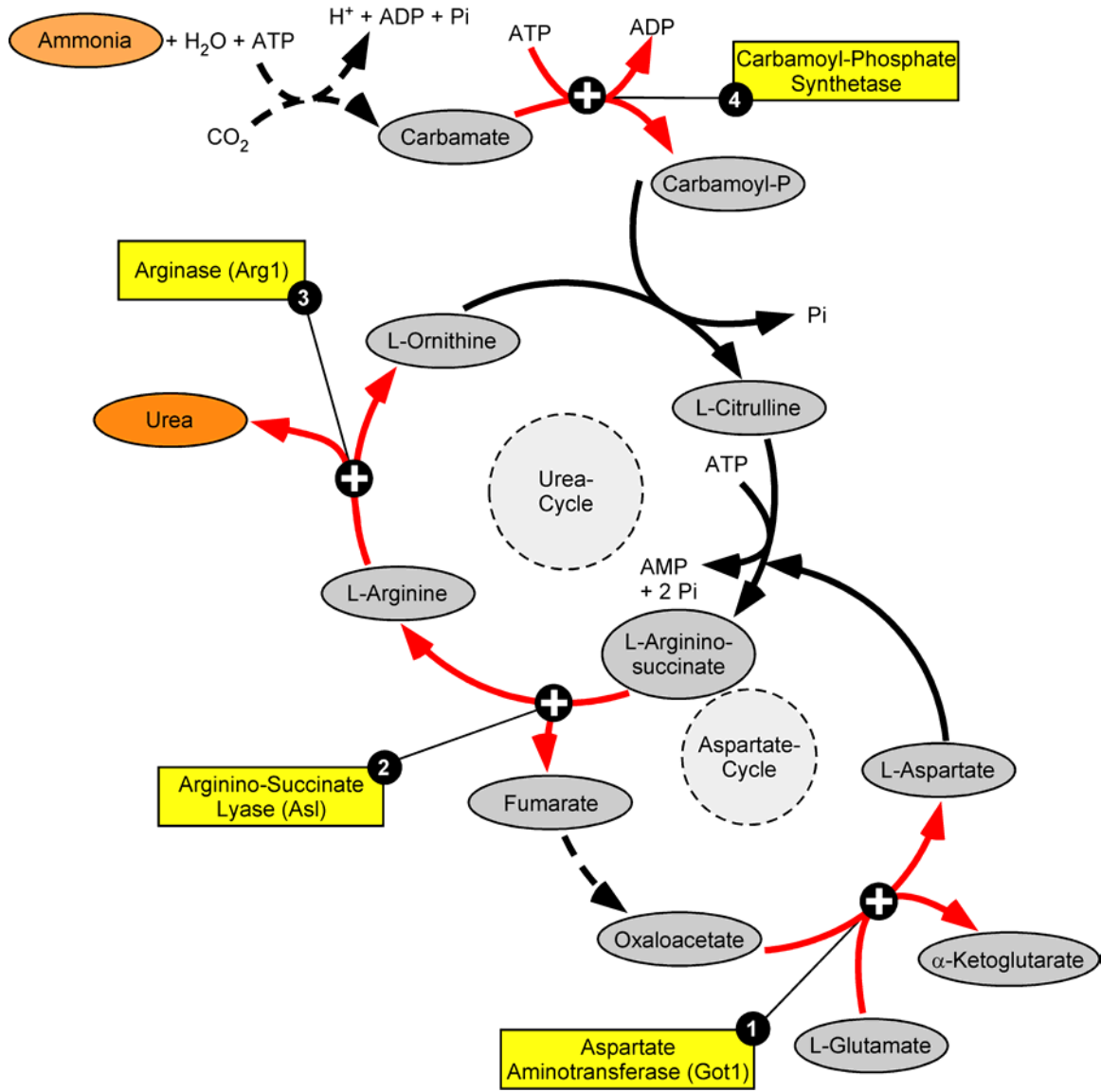


Figure 3

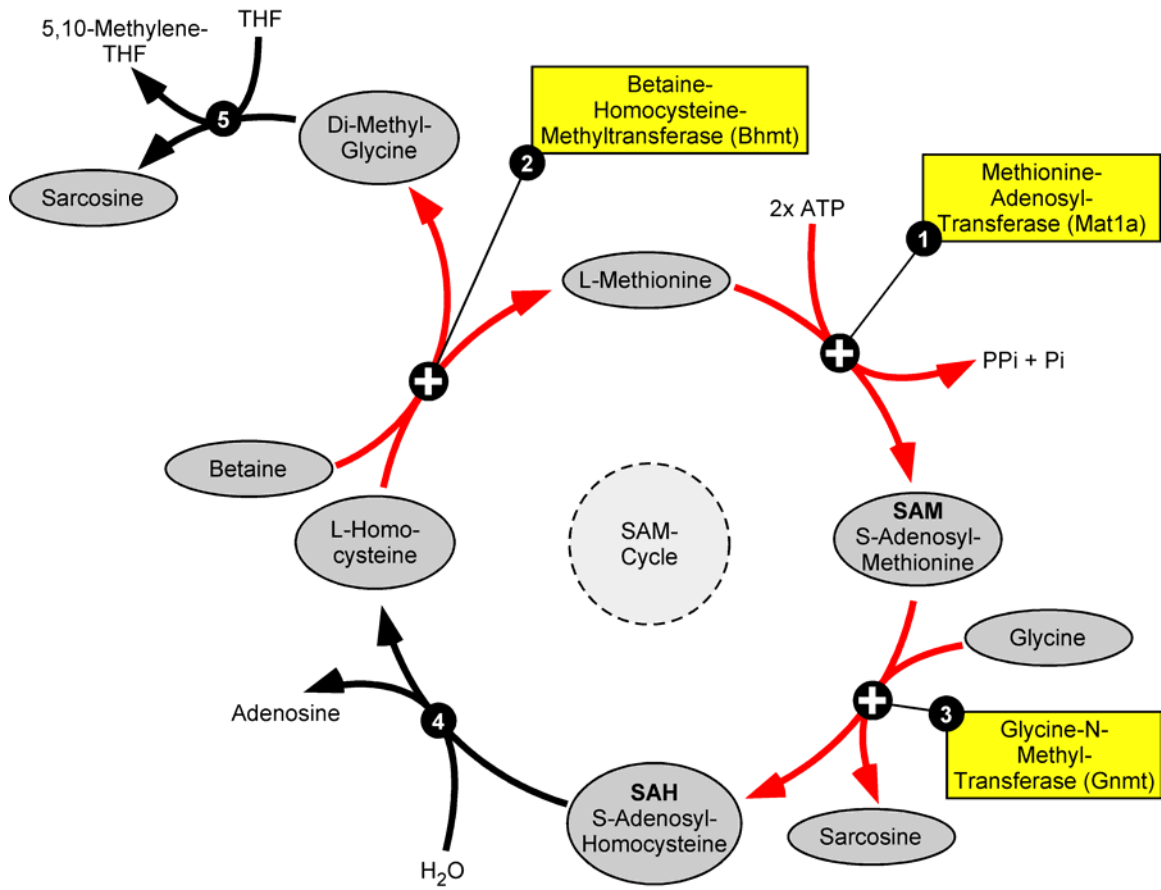


Figure 4

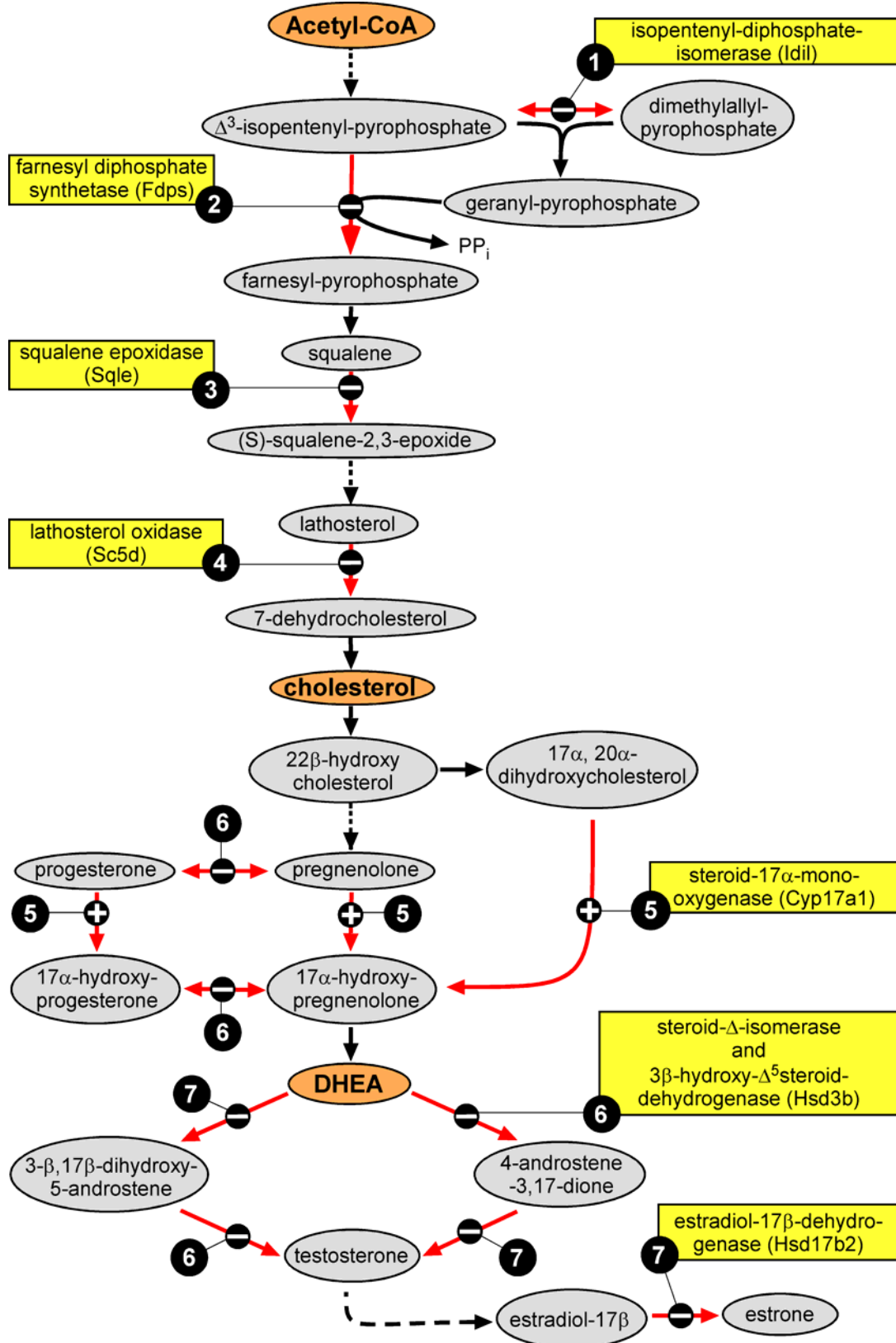


Figure 5

